

## Long-Range Flow-Induced Alignment of Self-Assembled Rosette Nanotubes on Si/SiO<sub>x</sub> and Poly(Methyl Methacrylate)-Coated Si/SiO<sub>x</sub>

Jose Raez, Jesus G. Moralez, and Hicham Fenniri\*

National Institute for Nanotechnology, National Research Council (NINT-NRC) and Department of Chemistry, University of Alberta, ECERF: 9107-116 Street Edmonton, Alberta T6G 2V4, Canada

Received September 11, 2004; E-mail: hicham.fenniri@nrc-cnrc.gc.ca

Nanotubular architectures are the topic of intense investigations as channels,<sup>1</sup> sensors,<sup>2</sup> reinforcers in polymer materials,<sup>3</sup> liquid crystals,<sup>4</sup> nanowires,<sup>5</sup> and medical implant materials.<sup>6</sup> In the absence of an external stimulus, these materials will be randomly oriented, thus affecting their bulk and nanoscopic properties. Microcontact printing,<sup>7</sup> magnetic<sup>8</sup> and electric<sup>9</sup> fields, lithographic techniques,<sup>10</sup> and directional flow methods<sup>11</sup> were used to orient carbon nanotubes (CNTs), and it was shown that their anisotropic electrical and thermal conductive properties depend on the degree and direction of their alignment.<sup>12</sup> While most of this work focused on CNTs, organic nanotubes, particularly those obtained through self-assembly,<sup>1,13</sup> remain unexplored.

The heteroaromatic bicyclic base G  $\wedge$  C undergoes hierarchical self-assembly in water to form a six-membered supermacrocycle maintained by 18 H-bonds (Figure 1). The resulting and substantially more hydrophobic nanodisks then self-organize to produce a tubular stack (rosette nanotubes, RNs) with tunable dimensions and properties.<sup>13</sup> Although maintained by weak intermolecular forces, these RNs can reach several micrometers in length on carbon-based or Si/SiO<sub>x</sub> surfaces. Their kinetic stability, processability, high aspect ratio, and chemical tunability offer numerous opportunities for applications in molecular electronics. A key step toward this goal is to develop reliable methods for the long-range organization of these materials on surfaces such that their properties can be fully explored in hybrid organo-silicon integrated devices. Here we report on (a) the long-range alignment of hydrophilic self-assembled RNs derived from modules **1** and **2** using directional flow<sup>14</sup> and (b) the effect of the surface on their morphology and stiffness.

The self-assembly of RNs has been previously established using transmission electron microscopy (TEM), dynamic light scattering, small-angle X-ray scattering, circular dichroism, and UV-vis melting studies.<sup>13</sup> Figure 2 shows TEM and AFM images of randomly oriented RNs obtained from **1** and **2** featuring a diameter of  $3.4 \pm 0.3$  nm, in agreement with the computed value of 3.5 nm. To align these nanotubes on a hydrophilic surface, a 30  $\mu$ L drop from a 1 mg/mL aqueous solution was deposited on a silicon substrate bearing a native oxide layer (Si/SiO<sub>x</sub>), resulting in immediate wetting of the surface. The substrate was then oriented vertically, and the fluid was allowed to flow under gravitational force. After the water was allowed to slowly evaporate, the surface was imaged by tapping mode-atomic force microscopy (TM-AFM). Figure 3 shows RNs aligned with the direction of the solution's flow. Comparison of Figures 2 and 3A,B shows that the directional flow method (a) induces dramatic morphological changes, (b) aligns the RNs along the direction of the flow, and (c) eliminates the formation of bundles and reduces entanglement. This result is attributed to the self-assembled nature of this material; the shear forces may lead to reversible breaking of the RNs, which then undergo self-assembly in an ordered fashion along the flow path. Although the alignment was prevalent across the entire substrate,

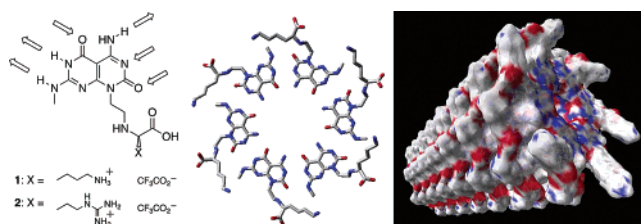


**Figure 1.** G  $\wedge$  C modules **1** and **2** and molecular model of self-assembled rosette (middle) and RN (right) obtained from **1** showing the electrostatic surface.

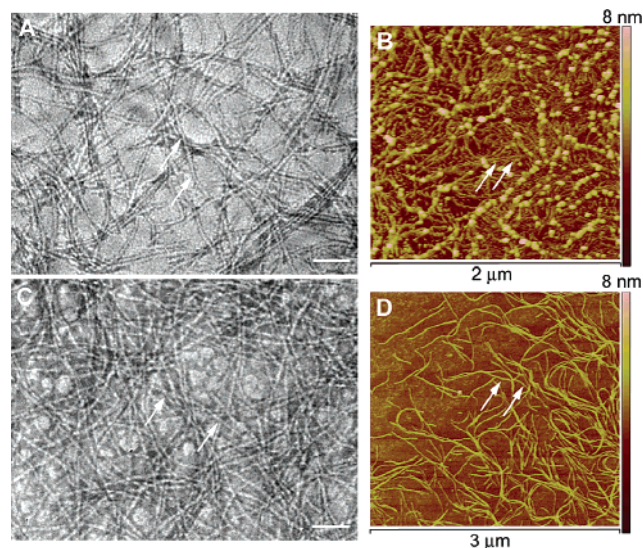


**Figure 2.** Negatively stained TEM micrographs (scale bar = 50 nm) and TM-AFM images (on Si/SiO<sub>x</sub>) of nonaligned RNs obtained from the self-assembly of **1** (A and B) and **2** (C and D). TEM samples were prepared by grid floating, and the AFM samples were prepared by spin coating (see Supporting Information for detail). Arrows point at individual RNs.

its degree depended on the nature of the self-assembling module, the flexibility of the resulting RNs, and the chemical nature of the surface. In general, 1D objects are more readily aligned when their contour length  $L$  is smaller than their persistence length  $l_p$ . An effective way to improve the alignment of flexible structures ( $L > l_p$ ) is by increasing their concentration, such that their lateral and rotational translations are minimized and their longitudinal translation is maximized as a result of packing. Thus, as anticipated, the alignment of RNs from a 5–10 mg/mL solution of **1** was improved although at the cost of significant bundling (Supporting Information).

To test the effect of the substrate's chemical properties on the directional flow method, the RNs were aligned on a Si/SiO<sub>x</sub> substrate coated with poly(methyl methacrylate) (PMMA). Due to the hydrophobic nature of PMMA (water contact angle =  $63.0 \pm$

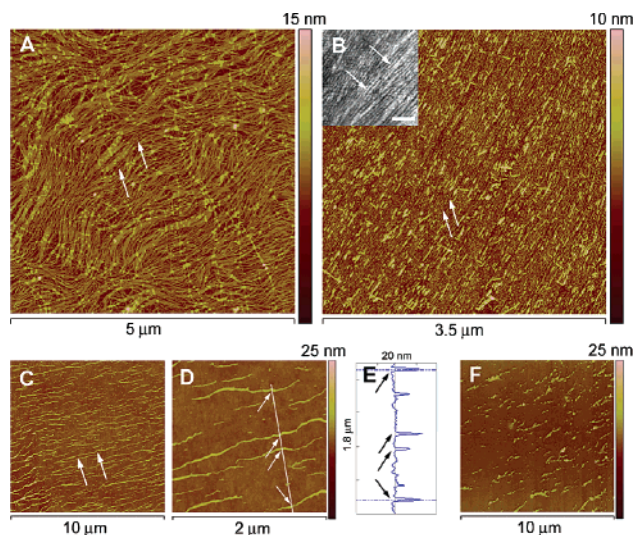


**Figure 3.** TM-AFM images of aligned RNs obtained from **1** and **2** on Si/SiO<sub>x</sub> and PMMA-coated Si/SiO<sub>x</sub> showing the surface effects on the aggregation behavior and degree of alignment of the RNs. (A) RNs (**1**) aligned on Si/SiO<sub>x</sub>. (B) RNs (**2**) aligned on Si/SiO<sub>x</sub>; the inset is a negatively stained SEM micrograph of the same sample (scale bar = 40 nm). (C) RNs (**1**) aligned on PMMA-coated Si/SiO<sub>x</sub>, and corresponding close-up image (D) and height profile (E). (F) RN (**2**) on PMMA-coated Si/SiO<sub>x</sub>. Arrows point at individual RNs.

0.9°), a 15  $\mu\text{L}$  droplet of RN (1 mg/mL aqueous solution) did neither wet the surface nor roll down when the substrate was oriented vertically. The alignment was therefore prompted mechanically using a plastic micropipet tip to move the droplet at a speed of 2 cm/min. TM-AFM imaging (Figure 3C–E) revealed, in the case of **1**, (a) alignment along the flow path, (b) lower coverage of the surface, (c) formation of bundled nanotubes and aggregates varying in height from 4.5 to 14.9 nm,<sup>15</sup> and (d) increased stiffness. Bundling combined with the high surface tension that PMMA exerts on the RNs increases the stiffness of the nanostructures. This concept has been well studied in the area of water–oil interfaces where the persistence length of the interface is severely affected by the interfacial tension that is exerted on it.<sup>16</sup> Although at this stage there are no theoretical models describing the effect of the substrate on the 2D aggregation behavior of self-assembled organic nanostructures, it is reasonable to postulate that unfavorable interactions between the charged RNs and PMMA lead to bundling, which increases stiffness and persistence length.

The chemical composition of the surface is also essential in the alignment and the structural preservation of self-assembled nanostructures. RNs obtained from **2** show increased stiffness and longer-range order on SiO/SiO<sub>x</sub> (compare Figure 3A and 3B), whereas on PMMA, the same preassembled nanotubes resulted in the formation of unstructured amorphous conglomerates varying in height from 4.3 to 22.4 nm (compare Figure 3B and 3F).<sup>15</sup> This behavior was attributed to a stronger multivalent interaction of the guanidinium groups with the methylesters of PMMA that could lead to disruption of the proposed electrostatic belt surrounding the RNs,<sup>13a</sup> and result in destabilization and disassembly. Conversely, RNs obtained from **1** maintained their structural integrity on PMMA (Figure 3C–E), albeit, with lower coverage, increased stiffness, and significant bundling. This behavior could be due to (a) an increased stability of the RNs assembled from **1**, (b) a weaker interaction of the

ammonium groups with the PMMA methylester groups, and/or (c) a higher propensity to form bundles to counteract the surface tension exerted by PMMA.

On the basis of these results, long-range alignment of RNs is feasible and demonstrates that the directional flow method is a reliable strategy for achieving long-range order of self-assembled dynamic nanostructures. Given the chemical tunability of the RNs' surface properties and relative ease of assembly, this system offers unique opportunities to probe the effect of substrate–nanotube interaction on the alignment process and electrical properties of the RNs. This work, along with other alignment methods (micro-contact printing, electric fields, microfluidic systems, lithographic techniques) on various surfaces (gold, titanium, graphite, mica), and molecular modeling studies will be reported in due course.

**Acknowledgment.** We thank NSERC, NRC, and the University of Alberta for supporting this program, and Dr. Motkuri Kishan for generating the molecular models. J.G.M. thanks NIH (GM55146-08) for a graduate fellowship.

**Supporting Information Available:** Experimental details and additional figures. This material is available free of charge via the Internet at <http://pubs.acs.org>.

## References

- (1) Bong, D. T.; Clark, T. D.; Granja, J. R.; Ghadiri, M. R. *Angew. Chem., Int. Ed.* **2001**, *40*, 988–1011.
- (2) Chen, R. J.; Choi, C. H.; Bangsaruntip, S.; Yenilmez, E.; Tang, W.; Wang, Q.; Chang, Y.-L.; Dai, H. *J. Am. Chem. Soc.* **2004**, *126*, 1563–1568.
- (3) Cadek, M.; Coleman, J. N.; Ryan, K. P.; Nicolosi, V.; Bister, G.; Fonseca, A.; Nagy, J. B.; Szostak, K.; Béguin, F.; Blau, W. J. *Nano Lett.* **2004**, *4*, 353–356.
- (4) (a) Jung, J. H.; John, G.; Yoshida, K.; Shimizu, T. *J. Am. Chem. Soc.* **2002**, *124*, 10674–10675. (b) Valéry, C.; Artzner, F.; Robert, B.; Gulick, T.; Keller, G.; Grabielle-Madelmont, C.; Torres, M.-L.; Cherif-Cheikh, R.; Paternostre, M. *Biophys. J.* **2004**, *86*, 2484–2501.
- (5) (a) Liu, D.; Park, S. H.; Reif, J. H.; LaBean, T. H. *Proc. Natl. Acad. Sci. U.S.A.* **2004**, *101*, 717–722. (b) Reches, M.; Gazit, E. *Science* **2003**, *300*, 625–627. (c) Tans, S. J.; Devoret, M. H.; Dai, H.; Thess, A.; Smalley, R. E.; Geerligs, L. J.; Dekker, C. *Nature* **1997**, *386*, 474–477.
- (6) Chun, A. L.; Moralez, J. G.; Fenniri, H.; Webster, T. J. *Nanotechnology* **2004**, *15*, S234–S239.
- (7) Tsurkruk, V. V.; Ko, H.; Peleshanko, S. *Phys. Rev. Lett.* **2004**, *92*, 065502 (1–4).
- (8) Smith, B. W.; Benes, Z.; Luzzi, D. E.; Fisher, J. E.; Walters, D. A.; Casavant, M. J.; Schmidt, J.; Smalley, R. E. *Appl. Phys. Lett.* **2000**, *77*, 663–665.
- (9) (a) Kumar, M. S.; Kim, T. H.; Lee, S. H.; Song, S. M.; Yang, J. W.; Nahm, K. S.; Suh, E. K. *Chem. Phys. Lett.* **2004**, *383*, 235–239. (b) Ural, A.; Li, Y.; Dai, H. *Appl. Phys. Lett.* **2002**, *81*, 3464–3466. (c) Ono, T.; Oesterschulze, E.; Georgiev, G.; Georgieva, A.; Kassing, R. *Nanotechnology* **2003**, *14*, 37–41. (d) Chen, X. Q.; Saito, T.; Yamada, H.; Matsushige, K. *Appl. Phys. Lett.* **2001**, *78*, 3714–3716.
- (10) Rao, S. G.; Huabg, L.; Setyawan, W.; Hong, S. *Nature* **2003**, *425*, 36–37.
- (11) (a) Lay, M. D.; Novak, J. P.; Snow, E. S. *Nano Lett.* **2004**, *4*, 603–605. (b) Shimoda, H.; Oh, S. J.; Geng, H. Z.; Walker, R. J.; Zhang, X. B.; McNeil, L. E.; Zhou, O. *Adv. Mater.* **2002**, *14*, 899–901.
- (12) (a) Hone, J.; Llaguno, M. C.; Nemes, N. M.; Johnson, A. T.; Fisher, J. E.; Walters, D. A.; Casavant, M. J.; Schmidt, J.; Smalley, R. E. *Appl. Phys. Lett.* **2000**, *77*, 666–668. (b) Wang, X.; Liu, Y.; Yu, G.; Xu, C.; Zhang, J.; Zhu, D. *J. Phys. Chem. B* **2001**, *105*, 9422–9425.
- (13) (a) Fenniri, H.; Mathivanan, P.; Vidale, K. L.; Sherman, D. M.; Hallenga, K.; Wood, K. V.; Stowell, J. G. *J. Am. Chem. Soc.* **2001**, *123*, 3854–3855. (b) Fenniri, H.; Deng, B.-L.; Ribbe, A. E. *J. Am. Chem. Soc.* **2002**, *124*, 11064–11072. (c) Fenniri, H.; Deng, B.-L.; Ribbe, A. E.; Hallenga, K.; Jacob, J.; Thiyagarajan, P. *Proc. Natl. Acad. Sci. U.S.A.* **2002**, *99*, 6487–6492.
- (14) Maubach, G.; Fritzsche, W. *Nano Lett.* **2004**, *4*, 607–611.
- (15) These are lower limits since TM-AFM tends to compress soft materials and results in lower height profiles: Kne, M.; Sumser, M. P.; Bittner, A. M.; Wege, C.; Jeske, H.; Hoffmann, D. M. P.; Kuhnke, K.; Kern, K. *Langmuir* **2004**, *20*, 441–447.
- (16) De Gennes, P. G.; Taupin, C. *J. Phys. Chem.* **1982**, *86*, 2294–2304.

JA044487D